The Journal of Experimental Biology 216, 2702-2712

doi:10.1242/jeb.085746

RESEARCH ARTICLE

A thermogenic secondary sexual character in male sea lamprey

Yu-Wen Chung-Davidson[1], M. Cody Priess[2], Chu-Yin Yeh[3], Cory O. Brant[1], Nicholas S. Johnson[1,*] Ke Li[1], Kaben G. Nanlohy[1], Mara B. Bryan[1,†], C. Titus Brown[4,5], Jongeun Choi[2,6] and Weiming Li[1,*,‡]

[1]Department of Fisheries and Wildlife, [2]Department of Mechanical Engineering, [3]Department of Physiology, [4]Department of Computer Science and Engineering, [5]Department of Microbiology and Molecular Genetics and [6]Department of Electrical and Computer Engineering, Michigan State University, East Lansing, MI 48824, USA

*Present address: USGS, Great Lakes Science Center, Hammond Bay Biological Station, 11188 Ray Road, Millersburg, MI 49759, USA
†Present address: Energy Biosciences Institute, University of California, Berkeley, 130 Calvin Laboratory, MC 5230, Berkeley, CA 94720, USA
‡Author for correspondence (liweim@msu.edu)

SUMMARY

Secondary sexual characters in animals are exaggerated ornaments or weapons for intrasexual competition. Unexpectedly, we found that a male secondary sexual character in sea lamprey (*Petromyzon marinus*) is a thermogenic adipose tissue that instantly increases its heat production during sexual encounters. This secondary sexual character, developed in front of the anterior dorsal fin of mature males, is a swollen dorsal ridge known as the 'rope' tissue. It contains nerve bundles, multivacuolar adipocytes and interstitial cells packed with small lipid droplets and mitochondria with dense and highly organized cristae. The fatty acid composition of the rope tissue is rich in unsaturated fatty acids. The cytochrome *c* oxidase activity is high but the ATP concentration is very low in the mitochondria of the rope tissue compared with those of the gill and muscle tissues. The rope tissue temperature immediately rose up to 0.3°C when the male encountered a conspecific. Mature males generated more heat in the rope and muscle tissues when presented with a mature female than when presented with a male (paired *t*-test, $P<0.05$). On average, the rope generated 0.027±0.013 W cm^{-3} more heat than the muscle in 10 min. Transcriptome analyses revealed that genes involved in fat cell differentiation are upregulated whereas those involved in oxidative-phosphorylation-coupled ATP synthesis are downregulated in the rope tissue compared with the gill and muscle tissues. Sexually mature male sea lamprey possess the only known thermogenic secondary sexual character that shows differential heat generation toward individual conspecifics.

Supplementary material available online at http://jeb.biologists.org/cgi/content/full/216/14/2702/DC1

Key words: *Petromyzon marinus*, electron transport chain, sea lamprey, sexual character, thermogenic, uncoupling protein.

Received 23 January 2013; Accepted 7 March 2013

INTRODUCTION

Lampreys are jawless vertebrates that diverged from jawed vertebrates 560 million years ago (Kumar and Hedges, 1998; Shu et al., 1999). The sea lamprey life cycle consists of larval, parasitic juvenile and anadromous adult stages (Applegate, 1950; Hardisty, 1979; Hardisty and Potter, 1971). At the final stage of sexual maturation, adult males develop a rope-like thickening at the dorsal ridge in front of their anterior dorsal fin (Fig. 1). Field observations have shown that mature males release a pheromone that attracts ovulatory females to their nest (Li et al., 2002), and often rub their rope tissue against the female abdomen. Females sometimes rub their urogenital pore on the rope tissue in return. After this initial courtship behavior, the male attaches onto the female's head with his oral disc and tightens a knot with his tail near the female urogenital pore. The spawning act ends with both partners thrusting vigorously to release gametes.

As the rope tissue appears to play an active role in the spawning act and is not merely an ornamental display, we examined the morphology and development of the dorsal ridge in sea lamprey. To our surprise, the morphology of the rope tissue consists of multivacuolar fat with interstitial fibroblast-like cells and collagen fibers. This finding led us to speculate that the rope tissue may be a primordial thermogenic fat. Many heat-generating organs or mechanisms have appeared along the evolution of vertebrates. Among the most well known is mammalian brown adipose tissue (BAT), which burns fatty acids to produce heat *via* uncoupling oxidative phosphorylation from ATP production in the mitochondria (Cannon and Nedergaard, 2004). However, outside of the mammalian clade the known heat-generating tissues are all derived from muscles (Cannon and Nedergaard, 2004). Birds, the other group of homeotherms, use muscles for nonshivering thermoregulation (Mozo et al., 2005). Several groups of fishes maintain brain temperatures higher than the environment by ATP-dependent Ca^{2+} cycling in the sarcoplasmic reticulum of 'heater cells' around the brain (Block, 1987). Therefore, the finding of a possible thermogenic fat was unexpected in non-mammalian species.

We examined whether the rope tissue exhibits characteristics of thermogenic fat through histological, chemical, biochemical, molecular biological, transcriptomic and behavioral analyses. We confirm that the rope tissue showed differential thermogenic ability toward individual conspecifics.

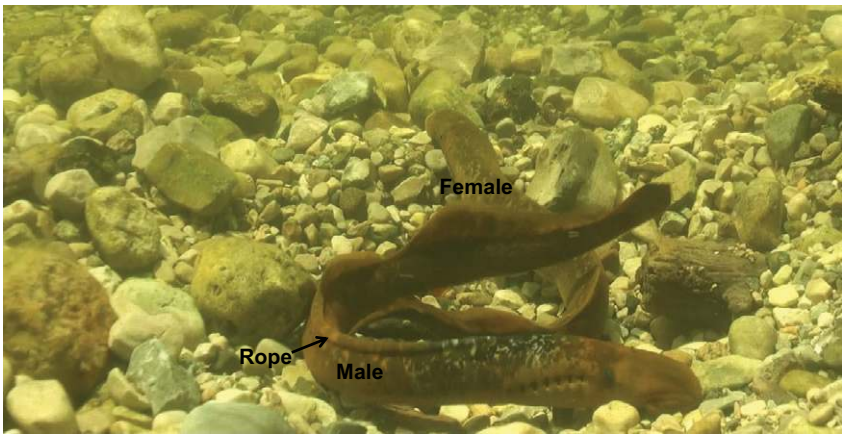

Fig. 1. Adult male sea lamprey develop a swollen dorsal ridge (rope tissue) in front of the anterior dorsal fin upon sexual maturation as a secondary sexual character. This photo, showing a male and a female sea lamprey in a nest, was taken by Cory O. Brant.

MATERIALS AND METHODS

Collection and maintenance of animals

Adult sea lampreys, *Petromyzon marinus* Linnaeus (body mass 200–350 g with an average body length of 48 cm), were captured during upstream spawning migration by agents of the US Fish and Wildlife Service and the Canada Department of Fisheries and Ocean from tributaries of Lakes Huron and Michigan. They were caged in streams until they completed final sexual maturation. Animal handling procedures were approved by the Institutional Animal Care and Use Committee at Michigan State University (MSU).

Fatty acid composition analyses (GC-MS)

Sea lamprey rope tissues were collected with the skin (epidermis) and underlying muscles carefully removed. Samples were snap frozen in liquid nitrogen and stored at −80°C before extraction. Rope tissue extracts (in dichloromethane) were methanolyzed at 100°C for 15 h. Fatty acid methyl esters were extracted with hexane and analyzed using an HP-5890A gas chromatograph with a 30 m×0.32 mm fused silica capillary column and eluted with helium at a 4°C min^{-1} increment in an oven starting at a temperature of 145°C and completed at 220°C. Chromatographic peaks were identified by comparing with a standard mixture containing 19 fatty acid methyl esters (GLC-68A, Nu-Chek Prep, Elysian, MN, USA).

Gene ontology analyses

Transcriptome expression data for sea lamprey rope, gill and muscle tissues were obtained using an Illumina Genome Analyzer II (Illumina, San Diego, CA, USA) and mRNA-Seq protocol (75-base) at the Research Technology Support Facility at MSU. Two-way BLASTX between lamprey transcriptome expressed sequence tags and mouse protein database was performed to obtain putative orthologies. Gene ontology (GO) categories were assigned to the corresponding expressed sequence tags according to NCBI/Entrez databases (http://www.ncbi.nlm.nih.gov/). Bowtie software was used to count the number of reads (Langmead et al., 2009). The raw counts were normalized using quantile normalization. Normalized profiles were pairwise-compared using GoMiner (Zeeberg et al., 2003). Heat maps were generated using CIMminer (Weinstein et al., 1997).

Histology and immunohistochemistry

Histology samples were processed in the Investigative Histopathology Laboratory, Department of Physiology and Human Pathology at MSU. Immunostaining for noradrenaline (NA) and uncoupling protein (UCP) followed methods described previously (Chung-Davidson et al., 2008). Negative controls (deprived of the NA or UCP antibody) were performed simultaneously in every immunostaining experiment. The antibody concentration used was 1:1000 for both NA (AB120, EMD Millipore, Billerica, MA, USA) and UCP-3 (U7757, reacted with an extract of rat BAT mitochondria; Sigma-Aldrich, St Louis, MO, USA).

Mitochondrial assays

Mitochondria were extracted from rope, gill and muscle tissues using a mitochondria isolation kit following the manufacturer's instructions (BioChain Institute, Newark, CA, USA). Briefly, 100 mg of rope, muscle and gill tissues from six mature males were dissected out and washed twice with 10 ml ice-cold 0.1 mol l^{-1} phosphate buffered saline (PBS; pH 7.4). Tissues were minced with small scissors in PBS on ice, and 1 ml 1× mitochondria isolation buffer was added. Tissues were then homogenized on ice for 20 s and held on ice for 5 s. Homogenization steps were repeated twice, and homogenates were centrifuged at 600 ***g*** at 4°C for 4 min. The supernatant was carefully transferred to a new tube and centrifuged at 12,000 ***g*** at 4°C for 15 min. The pellet was resuspended in 500 µl 1× mitochondria isolation buffer and serial centrifugation steps were repeated once. The pellet was resuspended in 100 µl isolation buffer or lysis buffer with 1× protease inhibitors. Protein concentration was measured using a microplate BCA protein assay kit (Thermo Fisher Scientific, Waltham, MA, USA).

Cytochrome *c* oxidase assays were performed using a mitochondria activity assay kit following the manufacturer's instructions (BioChain). Briefly, a colorimetric assay was used to measure mitochondria-specific cytochrome *c* oxidase activity in soluble or membrane-bound mitochondria samples as indicated by the oxidation of ferrocytochrome *c* to ferricytochrome *c* (absorbance at 550 and 565 nm, respectively). In this assay, cytochrome *c* was reduced with dithiothreitol and reoxidized by the active cytochrome *c* oxidase in the samples. The cytochrome *c* oxidase reaction is a first-order rate reaction with respect to the cytochrome concentration, showing an exponential decay over time. Therefore, we measured the initial fast reaction rate during the first 45 s of reaction using a kinetic program (5 s delay, 10 s interval, five readings: A_{5s}, A_{15s}, A_{25s}, A_{35s} and A_{45s}) in a spectrophotometer. A positive control (from the kit) was measured simultaneously. The integrity of the outer membrane was assessed by measuring cytochrome *c* oxidase activity in mitochondria membrane in the presence and absence of the detergent *n*-dodecyl-β-D-maltoside (from the kit). No damage of the mitochondrial outer membrane was found during our mitochondria preparation procedure.

ATP assays were performed using an ApoSENSOR ATP cell viability assay kit following the manufacturer's instructions

(BioVision, Milpitas, CA, USA). Briefly, rope, muscle and gill mitochondrial extracts and standards (0.1 ng ml^{-1} to 0.1 mg ml^{-1} in 10× serial dilution) were placed in a 96-well plate in triplicates and measured simultaneously in a GloMax 96 Microplate Luminometer (Promega, Madison, WI, USA). The assay utilized luciferase to catalyze the formation of light from ATP and luciferin. ATP concentration was measured before, immediately after (0 min) and 30 min after adding 2.5 mg ADP.

Phylogenetic tree analyses

The evolutionary history of the UCP proteins was inferred using the minimum evolution (ME) method. The optimal tree with the sum of branch length=5.46535823 is shown. The evolutionary distances were computed using the Jones–Taylor–Thornton (JTT) matrix-based method and are in the units of the number of amino acid substitutions per site. The ME tree was searched using the close-neighbor-interchange algorithm at a search level of 1. The neighbor-joining algorithm was used to generate the initial tree. All positions containing gaps and missing data were eliminated from the data set (complete deletion option). There were a total of 268 positions in the final data set. Phylogenetic analyses were conducted in MEGA4 (Tamura et al., 2007).

Real-time quantitative PCR

Real-time quantitative PCR (RT-qPCR) was performed using the TaqMan MGB system (Life Technologies, Carlsbad, CA, USA) as described previously (Chung-Davidson et al., 2008). Briefly, total RNA was extracted using TRIzol Reagent (Invitrogen, Carlsbad, CA, USA), treated with the TURBO DNA-free kit (Applied Biosystems, Foster City, CA, USA) and diluted to 100 ng µl^{-1}. RNA samples were then reverse-transcribed into cDNA using M-MLV reverse transcriptase (Invitrogen) and random primers (Promega). The reactions [2 µl (5 ng µl^{-1}) cDNA + 8 µl TaqMan Universal PCR mastermix with 900 nmol l^{-1} primers (each) and 250 nmol l^{-1} TaqMan RGB probes] were analyzed on an ABI 7900HT real-time PCR thermal cycler with the manufacturer's default setting (95°C for 10 min, 40 cycles of denature step: 95°C, 15 s, and anneal/extend step: 60°C, 1 min; MSU Genomics Technology Support Facility, East Lansing, MI, USA). Synthetic oligos were used as standards and run on the same 384-well plate with the samples. Standards were PCR-amplified using the primers for RT-qPCR, purified with the MinElute PCR purification kit (Qiagen, Valencia, CA, USA, and serially diluted (10-fold) into 10^{10} to 10^{3} molecules per 2 µl solution. The sequences for standards, primers and TaqMan MGB probe for each mRNA are listed in supplementary material Appendix S1.

Temperature measurement and behavioral recording

Mature male sea lamprey were anesthetized with 0.02% MS222 (Sigma-Aldrich), wrapped with a wet cloth around the gill openings, and temporarily removed from the water for surgery. Small 5 mm incisions were cut at the center of the rope tissue and the muscle tissue on the side of the body. Miniature waterproof temperature probes (diameter 3.175 mm, ON-402-pp; Omega Engineering, Stamford, CT, USA) were sutured into the rope and muscle tissues and sealed with VetBond (3M, St Paul, MN, USA). Animals were immediately placed in a behavioral observation tank (122×122×89 cm, length × width × height) after surgery. After the lamprey recovered from the anesthesia and the rope and muscle temperatures returned from the ambient air temperature to the water temperature, individual mature females or males were placed in the same tank to observe their behavioral and temperature changes for 10 min. Temperature

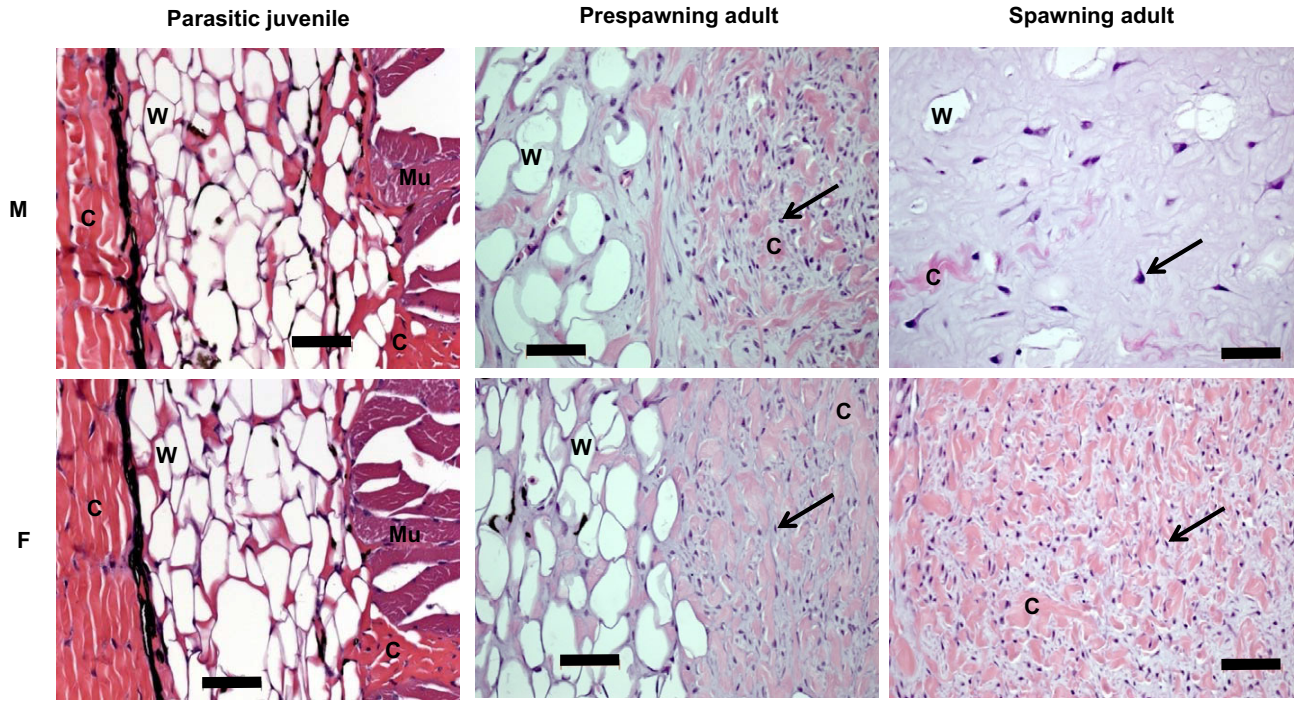

Fig. 2. Cellular morphology of the dorsal ridge of juvenile and adult sea lamprey (hematoxylin and eosin stain). The dorsal ridge in parasitic juveniles contains only white adipocytes (W); in sexually immature adults, both white adipocytes and interstitial fibroblast-like cells (arrows) are present. In mature adults, these interstitial fibroblast-like cells replace white adipose tissue in the dorsal ridge, and display robust sexual dimorphism. Note that the dorsal ridge of mature males contains large adipocytes and interstitial fibroblast-like cells, whereas the dorsal ridge of mature females contains only small interstitial fibroblast-like cells and many collagen fibers (C). F, female; M, male; Mu, muscle. Scale bars, 50 µm.

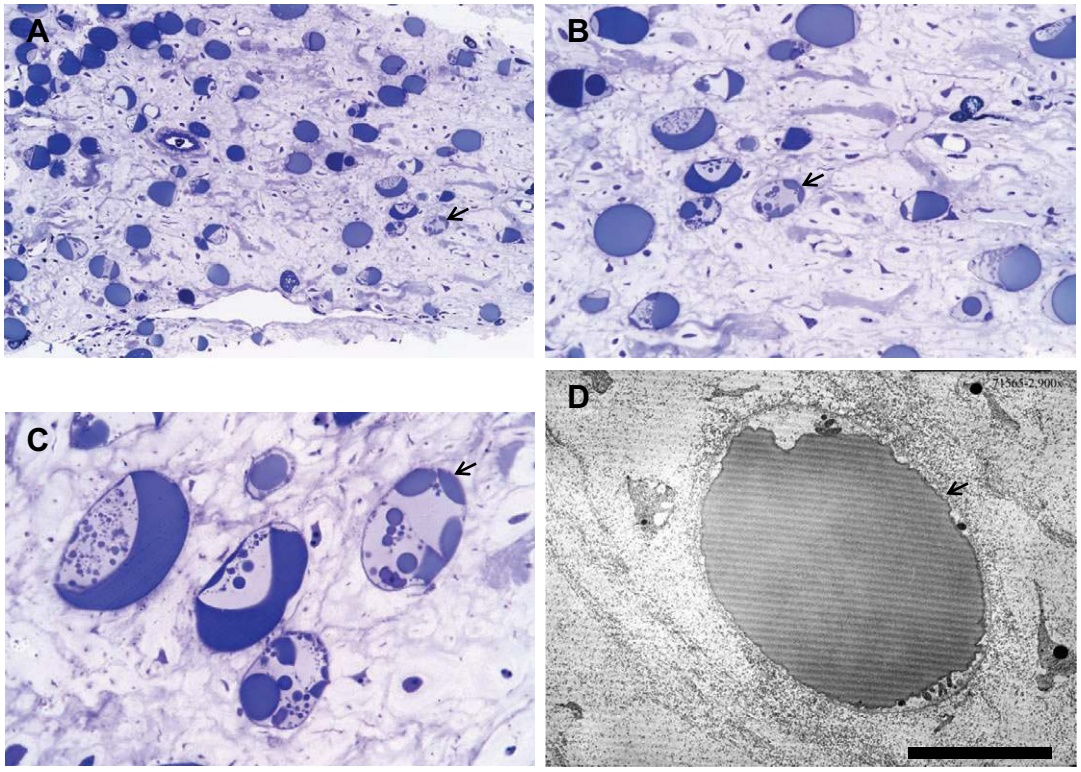

Fig. 3. Cellular morphology and the ultrastructure of the multivacuolar adipocytes in the rope tissue of mature male sea lamprey. (A) Toluene-Blue-stained adipocytes with multiple oil droplets (indicated by a black arrow) in the rope tissue (40× micrograph). (B) Toluene-Blue-stained adipocytes with multiple oil droplets (indicated by a black arrow) in the rope tissue (100× micrograph). (C) Toluene-Blue-stained adipocytes with multiple oil droplets (indicated by a black arrow) in the rope tissue (400× micrograph). (D) Transmission electron micrograph of the multivacuolar adipocyte in the rope tissue. Scale bar, 50 µm.

readings were simultaneously recorded from the water, rope and muscle tissues using three handheld thermistor thermometers (ultra-high-accuracy: ±0.015°C, resolution: 0.01°C, range: −20 to ~130°C, HH41, Omega Engineering). Lamprey behaviors were recorded using a Sony HDR-CX550V video camera (New York, NY, USA) enclosed in an Ikelite custom underwater housing equipped with an Ikelite WP80 wide-angle lens (Indianapolis, IN, USA). The VetBond seal remained intact for a few hours. Once water leaked into the tissue (as determined by a temperature drop to the same level as water temperature), behavioral and temperature recordings were paused or stopped. In some cases, the behavioral and temperature recordings were resumed after reapplication of VetBond.

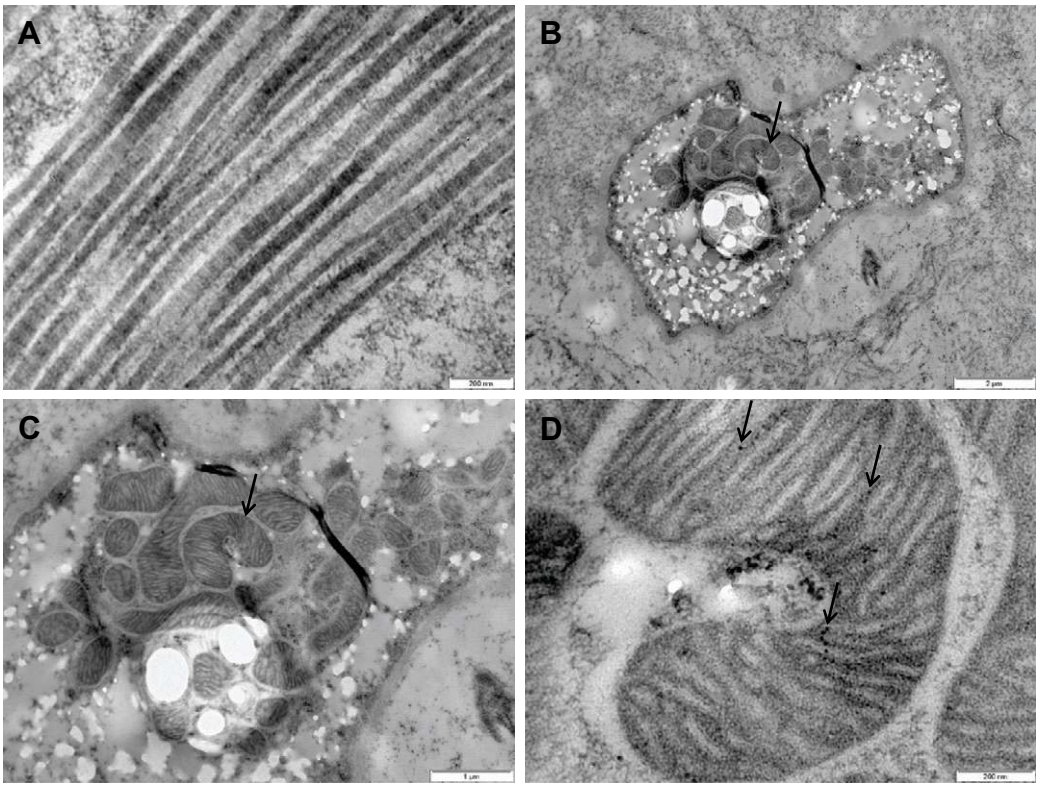

Fig. 4. The ultrastructure of the collagen fiber (A) and interstitial fibroblast-like cell (B–D) in the rope tissue. (A) Transmission electron micrograph of the collagen fibers in the rope tissue. Scale bar, 200 nm. (B) Transmission electron micrograph showing an interstitial fibroblast-like cell packed with mitochondria (arrow) with dense cristae and small lipid droplets in the rope tissue. Scale bar, 2 µm. (C) Transmission electron micrograph of the same mitochondria (arrow) shown in B at higher magnification. Scale bar, 1 µm. (D) Transmission electron micrograph showing UCP-immunogold (10 nm, indicated by arrows) in a mitochondrion of an interstitial fibroblast-like cell of the rope tissue. Scale bar, 200 nm.

Transmission electron microscopy

Fixed tissues were processed for transmission electron microscopy (TEM) in the Center for Advanced Microscopy at MSU. Ultrathin sections were blocked with normal goat serum (Vector, Burlingame, CA, USA) at room temperature for 1 h, incubated in a mixture of antibody for UCP-3 (1:1000, reacted with an extract of rat BAT mitochondria; Sigma-Aldrich) and normal goat serum (Vector) at room temperature for 1 h. Ultrathin sections were then incubated in goat-anti-rabbit IgG-10 nm gold (1:100, Sigma-Aldrich) for 1 h at room temperature. Transmission electron micrographs were taken with a JEOL100CXII (JEOL USA, Peabody, MA, USA).

RESULTS

Sexual dimorphism in the dorsal ridge of mature sea lamprey

We first examined the morphology and development of the dorsal ridge in sea lamprey at various developmental stages (Fig. 2; supplementary material Fig. S1). The dorsal ridge in parasitic juveniles contains only white adipose tissue (WAT). A structure containing interstitial fibroblast-like cells developed within the WAT in sexually immature migratory adults. The rope tissue of mature males contains large interstitial fibroblast-like cells and huge adipocytes with multiple oil droplets (Figs 2, 3), whereas the dorsal ridge of mature females contains only small interstitial fibroblast-like cells and many collagen fibers (Fig. 2, Fig. 4A). Therefore, the dorsal ridge in mature adults exhibits robust sexual dimorphism.

Characteristics of the rope tissue in mature male sea lamprey

To seek an explanation for the function of these male-specific interstitial cells, we investigated their ultrastructure using TEM and immunogold staining. The interstitial fibroblast-like cells in the rope tissue were packed with small oil droplets and mitochondria with highly organized cristae that spanned the entire width of the mitochondria (Fig. 4B–D). The inner membrane of the rope mitochondria (Fig. 4D) contained immunoreactivities for UCPs, which could be induced by androstenedione (Fig. 5), a sea lamprey androgen (Bryan et al., 2007). Several unmyelinated nerve bundles were also present in the rope tissue (supplementary material Fig. S2). However, enriched vasculature, a characteristic of mammalian BAT (Cannon and Nedergaard, 2004), was not observed in sea lamprey rope tissue. Enriched vasculature transfers heat away from mammalian BAT to maintain whole-body homeostasis (Cannon and Nedergaard, 2004). Because the sea lamprey is ectothermic, such vasculature is not necessary for thermoregulation of the whole body and the generated heat could be confined in the rope tissue.

We then measured the fatty acid composition of the rope tissues (Fig. 6) and found fatty acids present similar to those in mammalian BAT (Ohno et al., 2001). Interestingly, the relative abundance of docosahexaenate (C22:6), which correlates with the oxygen consumption, thermogenic activity and proliferation of BAT (12), was three times higher in the rope tissue than in mammalian BAT. Sea lamprey rope tissue also contained pentadecanoate (C15:0), hexadecadienoate (C16:2), margarate (C17:0), heptadecenoate (C17:1) and arachidate (C20:0), which had not been observed in mammalian BAT (Ohno et al., 2001).

Sea lamprey rope tissue is thermogenic

Because the rope tissue showed some morphological and biochemical hallmarks of BAT, we suspected that the rope tissue might be thermogenic. In mammalian BAT mitochondria, uncoupling protein 1 (UCP-1) is known to uncouple ATP production and dissipate proton-motive force as heat (Cannon and Nedergaard,

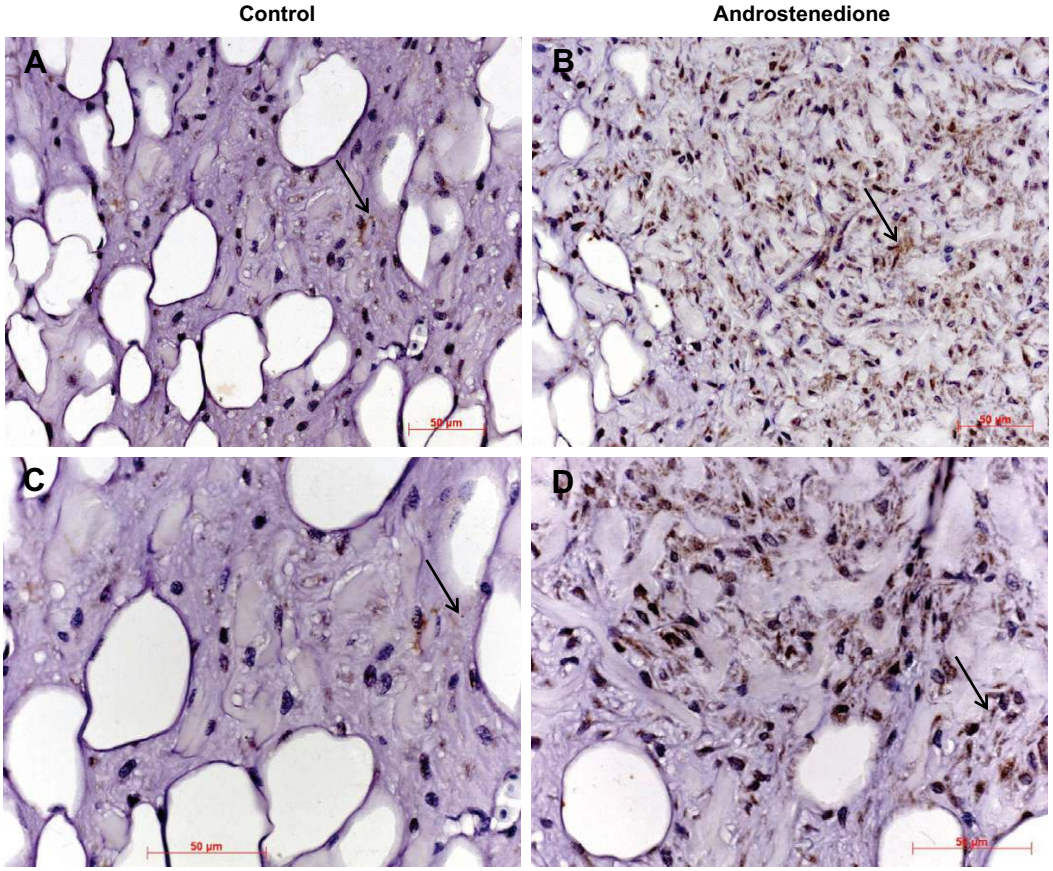

Fig. 5. Uncoupling protein (UCP) immunoreactivity in the rope tissue of mature male sea lamprey. (A,C) Immunostaining (brown, indicated by a black arrow) of UCP in the rope tissue of a control male. (B,D) UCP immunostaining (brown, indicated by a black arrow) is induced in the rope tissue of an androstenedione-treated male. Sections were counterstained with hematoxylin (purple/blue stain).

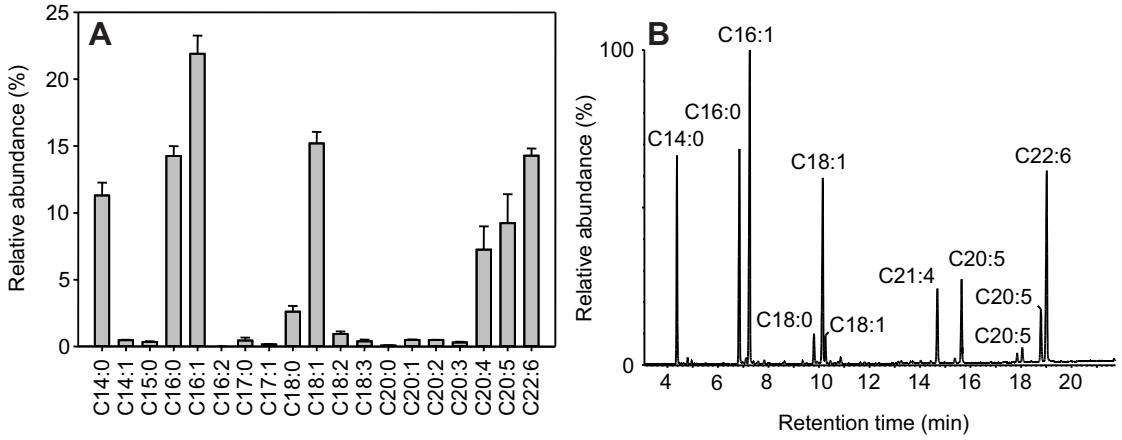

Fig. 6. Fatty acid composition of sea lamprey rope tissues. (A) Relative abundance of fatty acids. Fatty acid identity; C14:0 myristate, C14:1 myristolate, #C15:0 pentadecanoate, C16:0 palmitate, C16:1 palmitoleate, #C16:2 hexadecadienoate, #C17:0 margarate, #C17:1 heptadecenoate, C18:0 stearate, C18:1 oleate, C18:2 (n-6) linoleate, C18:3 (n-3) linolenate, #C20:0 arachidate, C20:1 gadoleate, C20:2 eicosadienoate, C20:3 (n-6) bis-homo-γ-linolenate, C20:4 (n-6) arachidonate, C20:5 (n-3) eicosapentaenoate, C22:5 (n-6) docosapentaenoate, C22:6 (n-3) docosahexaenoate. #, not present in mammalian brown adipocytes. Data represent means ± s.e.m. of three replicates. (B) A GC/MS chromatograph of the rope tissue.

2004). To determine whether ATP production is low in the UCP-laden rope tissue mitochondria, we measured the cytochrome *c* oxidase activity and ATP concentration in the mitochondria from rope, gill and muscle tissues. Cytochrome *c* oxidase is the last enzyme in the electron transport chain and an indicator of respiratory activity. Gill and muscle were chosen for their enriched mitochondria and high levels of respiratory activities. The specific activity of cytochrome *c* oxidase in rope tissue mitochondria was 5.7- and 3.0-fold higher than in gill and muscle tissue, respectively [ANOVA, $P<0.01$; Fisher's protected least significant difference (PLSD) *post hoc* tests: rope *versus* gill, $P<0.005$; rope *versus* muscle, $P<0.05$; Fig. 7A]. In contrast, ATP concentration was much higher in the gill and muscle but minimal in the rope tissue mitochondria (one-way ANOVA for repeated measures, $P<0.01$; Fisher's PLSD *post hoc* tests: rope *versus* gill, $P<0.0005$; rope *versus* muscle, $P<0.05$; Fig. 7B). These results suggest that oxidative phosphorylation may be uncoupled from ATP production in the rope tissue. However, the actual mechanisms remain to be confirmed.

To test directly the thermogenic capacity of the rope tissue, we measured the temperature of the rope and muscle tissues of mature males ($N=12$) in the presence of conspecific individuals (mature female *versus* mature male). The water temperature was recorded simultaneously as a reference. Muscle tissues were chosen as a control because of their thermogenic ability. We estimated the heat generation using free convection as the primary heat transfer method (Lepria et al., 2003) and modeled the rope and muscle tissues as a long cylinder with uniform volumetric heat generation (supplementary material Appendix S2). Fig. 8 shows the recordings from a mature male responsive to different partners and a mature male non-responsive to conspecifics examined. Table 1 presents the average measures of the maximum, minimum and mean temperature difference and the heat production over 10 min, from 12 mature males exposed to different partners. The rope tissue generated 0.027±0.013 W cm^{-3} more heat than the muscle (paired *t*-test, $P<0.05$) in 10 min. The specific heat production of the rope tissue was higher than muscle in every situation (Table 1; supplementary material Appendix S2). Interestingly, mature males generated more heat in the rope and muscle tissues when they encountered a mature female than a mature male (paired *t*-test, $P<0.05$). Individual males also showed variation in the amount of heat generated in the rope and muscle tissues in response to different mature females. The specific thermogenicity per unit weight by sea lamprey rope tissue is comparable to the energy expenditure per unit weight of BAT, estimated as the metabolic difference between UCP-1 knockout and wild-type mice (McDaneld et al., 2002). The most

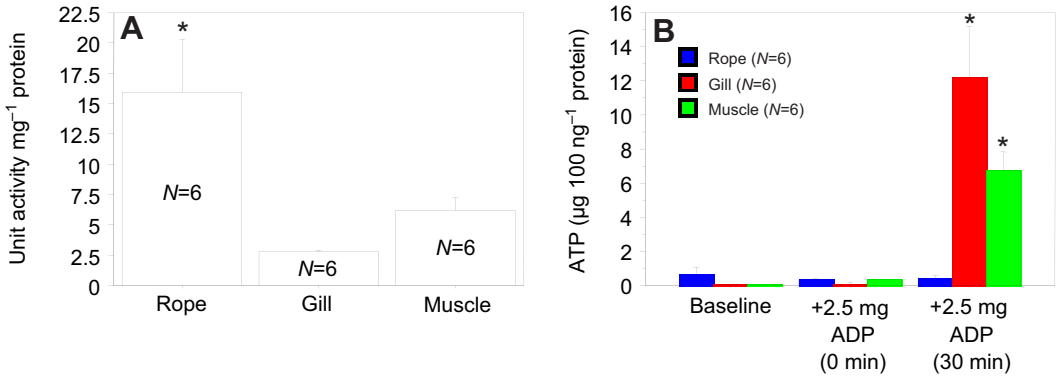

Fig. 7. Biochemical analyses of the mitochondrial extracts from the rope, gill and muscle tissues of mature male sea lamprey. (A) Specific activities of mitochondrial cytochrome *c* oxidase from the rope, gill and muscle tissues. (B) ATP concentrations measured from the same mitochondrial extracts shown in A. ATP concentration was measured prior to ADP addition (baseline), immediately after adding 2.5 mg ADP (0 min), and 30 min after adding 2.5 mg ADP.

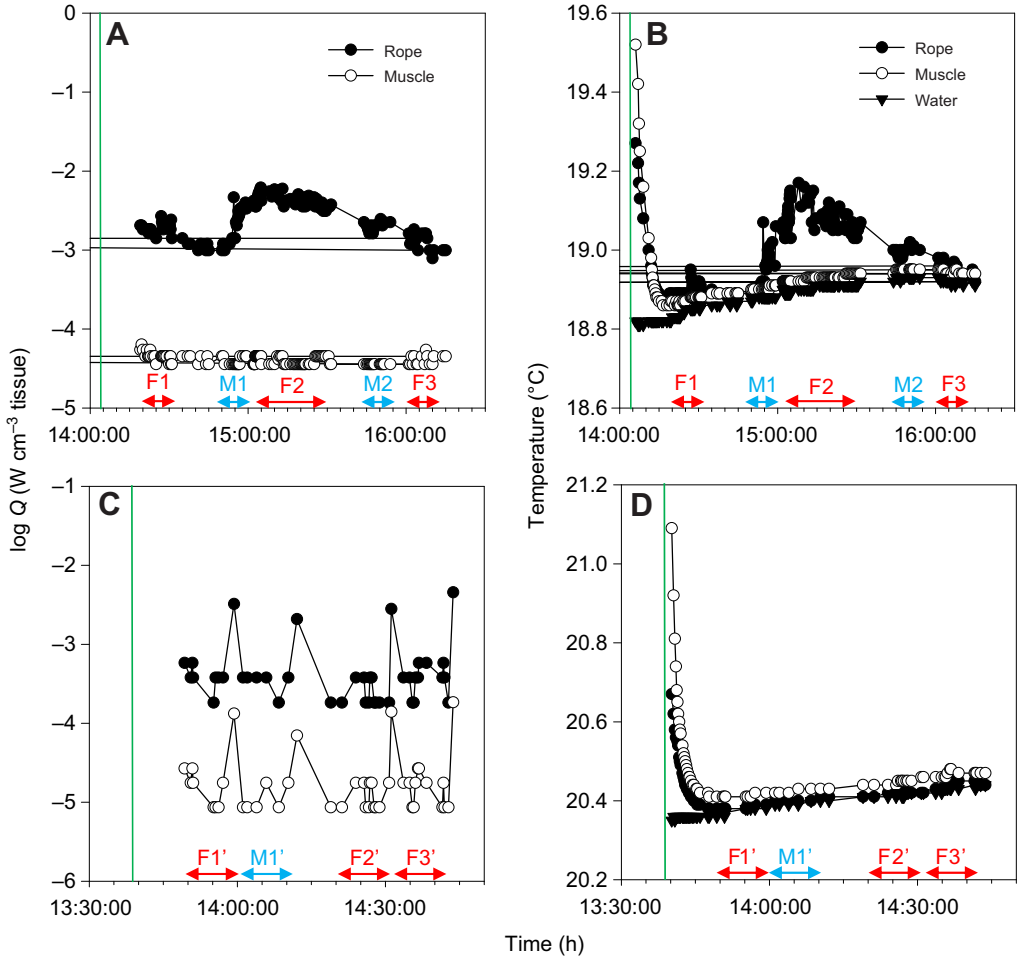

Fig. 8. Time course of the heat production (Q) and temperature change of the rope tissue (solid circle) and muscle (open circle) in a mature male responsive (A,B) and non-responsive (C,D) to male and female conspecifics examined. Water temperature (solid triangle) was recorded simultaneously. Arrows highlight the time periods with different partners. F, female; M, male. Numbers represent different individuals. Green line indicates the time point when the animal was placed in the aquarium after surgery. Note that the high temperatures of the rope and muscle tissues at the beginning were due to the exposure to ambient air temperature during surgery.

dramatic observation in this study was that the rope tissue temperature rose by up to 0.3°C immediately after sexual encounter (Fig. 8).

The rope tissue is under adrenergic neural control

Based on the instant heat generation by the rope tissue in response to potential mates, we reasoned that the rope tissue is under adrenergic neural control, as in mammalian BAT (Cannon and Nedergaard, 2004). We examined whether sea lamprey rope tissue contained NA. As expected, although the dorsal ridge of immature adults contained NA-immunoreactive fibers in both sexes, only mature males showed NA immunoreactivity in the rope tissue (Fig. 9). The dorsal ridge of mature females was not NA-

Table 1. Temperature difference and heat production in the rope and muscle tissues of mature male sea lamprey with partners of different sex

	Rope		Muscle		ΔRope–Muscle	
	OF	MM	OF	MM	OF	MM
T_{max} (°C)	0.076±0.024*	0.047±0.016	0.037±0.004*	0.021±0.004	0.040±0.020*	0.026±0.014
T_{min} (°C)	0.008±0.004	0.012±0.005*	–0.002±0.005	0.001±0.006*	0.010±0.006	0.011±0.004*
T_{mean} (°C)	0.033±0.009*	0.029±0.008	0.016±0.004*	0.009±0.004	0.017±0.007	0.020±0.006*
Q_{max} (W cm^{-3})	0.056±0.030*	0.022±0.008	0.002±0.001*	0.001±0.000	0.053±0.029*	0.021±0.008
Q_{min} (W cm^{-3})	0.012±0.004	0.018±0.006*	0.000±0.000	0.000±0.000	0.010±0.004	0.017±0.006*
Q_{mean} (W cm^{-3})	0.029±0.013*	0.020±0.007	0.002±0.001*	0.001±0.000	0.027±0.013*	0.019±0.007

Data are presented as means ± s.e.m. (N=12). T_{max}, T_{min} and T_{mean} are the maximum, minimum and mean temperature difference between the tissue and water (T_{tissue}–T_{water}). Q_{max}, Q_{min} and Q_{mean} are the maximum, minimum and mean heat production for 10 min. ΔRope–Muscle is the difference between the rope and muscle tissues. Paired t-tests and Fisher's R-to-Z-tests were performed to compare the parameters in the presence of partners of different sex [ovulatory female (OF) *versus* mature male (MM)]. Asterisks indicate significantly higher values in the presence of one sex *versus* the other (*P<0.05).

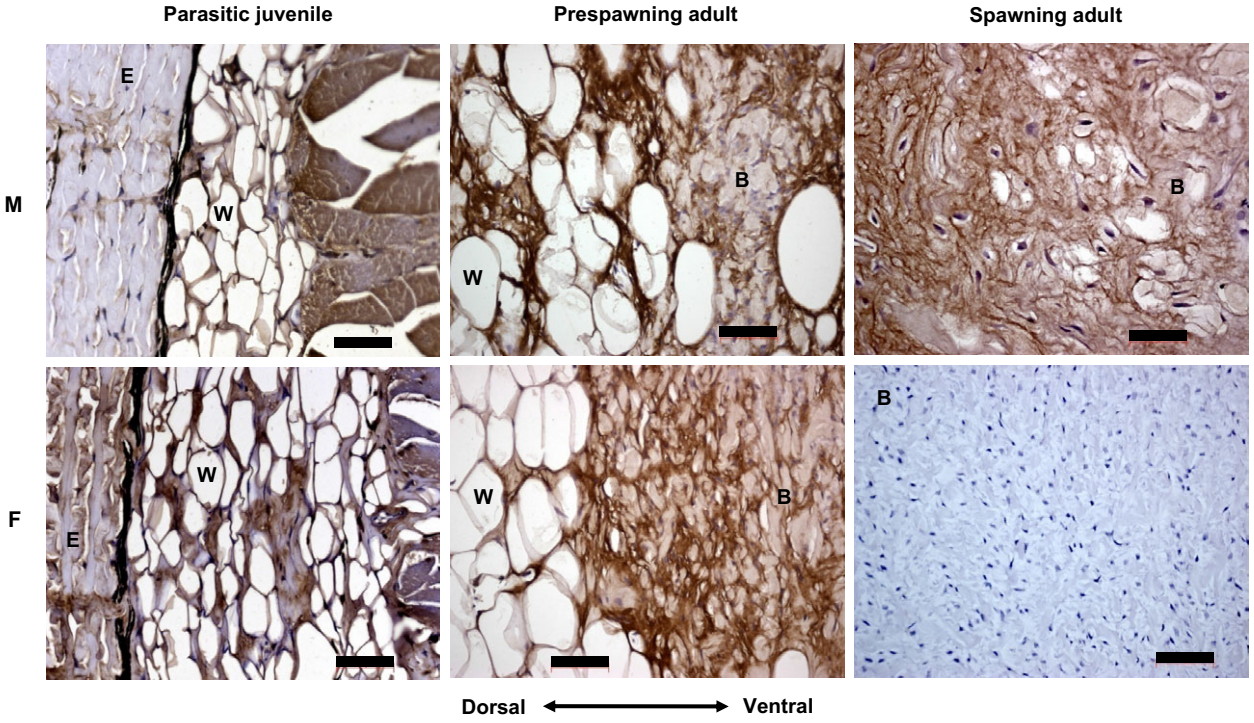

Fig. 9. Sexual dimorphism of noradrenaline (NA) immunoreactivity in sea lamprey dorsal ridge. NA immunohistochemistry (brown stain) was performed on the tissues from the dorsal ridge of lamprey in various life stages. Sexual dimorphism of NA immunoreactivity was observed in the dorsal ridge of mature adults. Sections were counterstained with hematoxylin (blue/purple nuclear stain). B, thermogenic adipose tissue; E, epidermis; F, female; M, male; W, white adipose tissue. Scale bars, 50 µm.

immunoreactive (Fig. 9). Our results are consistent with reports that NA fibers innervate BAT, forming a dense network within the tissue that is in contact with each brown adipocyte (Cannon and Nedergaard, 2004). The sexual dimorphism in NA immunoreactivities could also be a developmental factor responsible for the dimorphic morphology, as NA is a recruiting signal of brown adipogenesis in mammals (Cannon and Nedergaard, 2004; Farmer, 2008; Gesta et al., 2007).

Transcriptional control of rope tissue adipogenesis

To further elucidate the male-specific adipogenesis in the dorsal ridge, we examined the expression of several developmental markers, PR domain containing 16 (PRDM16), peroxisome proliferator-activated receptor γ (PPARγ), peroxisome proliferator-activated receptor gamma coactivator 1-alpha (PGC-1α), CCAAT-enhancer-binding protein (C/EBP), necdin and UCP in rope, gill and muscle tissues (Fig. 10). PRDM16 expression is essential for progenitor cells to

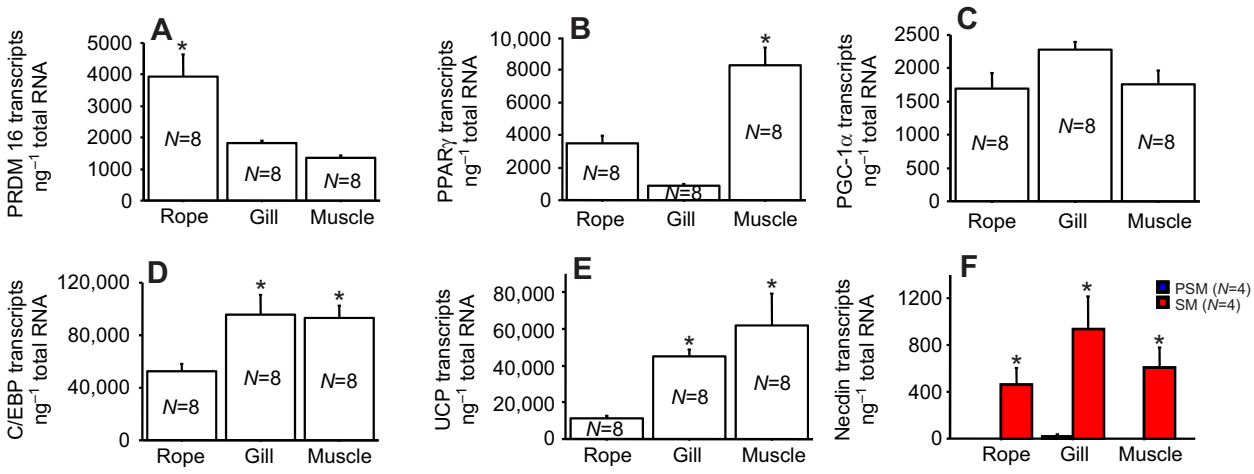

Fig. 10. Real-time quantitative PCR analyses of various genes in the rope tissue. (A) PRDM16, a brown adipose tissue (BAT) marker, is highly expressed in the rope tissue compared with gill and muscle. (B) PPARγ, a transcription factor, is highly expressed in muscle tissue compared with the gill and rope tissues. (C) PGC-1α, a downstream transcription factor of PPARγ, is not differentially expressed in the rope, gill or muscle tissues. (D) C/EBP, a downstream transcription factor of PGC-1α, is highly expressed in gill and muscle compared with rope tissue. (E) UCP is highly expressed in gill and muscle compared with rope tissue. (F) Necdin, an inhibitory factor for BAT development, is only expressed in mature males (SM) but not in immature males (PSM). Data represent means ± s.e.m. Sample size (*N*) is shown in the graphs. *Significant difference ($P<0.05$) from other groups.

A

MVGLRPTDVPPTAAVKFIGAGTAACIADLITFPLDTAKVRLQVQGECQRG
EGAARSAGVQYRGVFGTIAAMVRTEGPRSLYSGLVAGLQRQMSFASVRIG
LYDSVKNFYTNGAEHAGIGCRLLAGCTTGAMAVTFAQPTDVVKVRFQAQV
NMLGTSKRYSGTMNAYKTIAREEGVRGLWKGTGPNITRNAIVNCAELVTY
DIIKDTILKYKLLTDNLPCHFVSAFGAGFCTTVVASPVDVVKTRYMNSAP
GQYRSAFNCAYLMLTKEGAMAFYKGFVPSFLRLGSWNVVMFVTYEQLKRG
IMMAKQSWEKEVVFGPPTVRRSVHVTKHGNGGRVVQDISSNRTTTHGKHF
ARNNYSSR

B

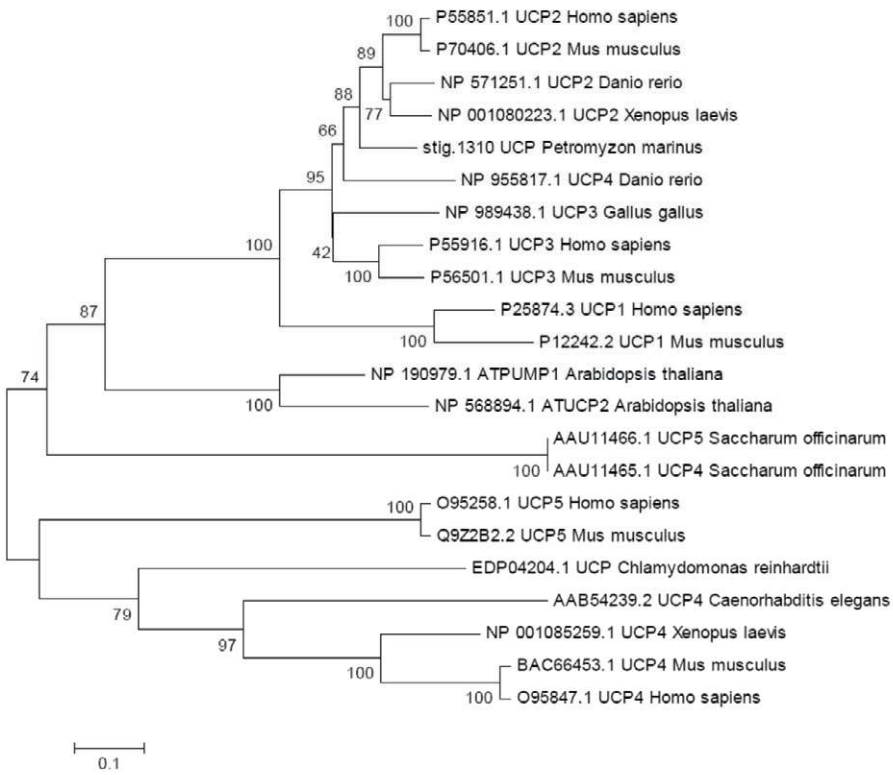

Fig. 11. Phylogenetic analysis of the sea lamprey UCP sequence. (A) Sea lamprey UCP sequence. Highlighted regions show three 'energy transfer protein signatures'. The amino acids (L, V) involved in pH sensing of the nucleotide binding site are underlined. Potential nucleotide binding sites are outlined. (B) A phylogenetic tree of selected UCPs. The evolutionary history was inferred using the minimum evolution (ME) method. The optimal tree with the sum of branch length=5.46535823 is shown. The percentage of replicate trees in which the associated taxa clustered together in the bootstrap test (1000 replicates) is shown next to the branches. The tree is drawn to scale, with branch lengths in the same units as those of the evolutionary distances used to infer the phylogenetic tree. The evolutionary distances were computed using the JTT matrix-based method and are in the units of the number of amino acid substitutions per site. The ME tree was searched using the close-neighbor-interchange algorithm at a search level of 1. The neighbor-joining algorithm was used to generate the initial tree. All positions containing gaps and missing data were eliminated from the data set (complete deletion option). There were a total of 268 positions in the final data set.

assume the brown adipocyte lineage in mammals (Farmer, 2008; Hansen and Kristiansen, 2006; Seale et al., 2007). PPARγ, PGC-1α and C/EBP are downstream transcription factors that induce UCP expression in mammalian BAT (Seale et al., 2007). Necdin serves as an inhibitor in the process of mammalian brown adipogenesis (Seale et al., 2007). We searched for these markers in the sea lamprey draft genome 2.0 (Libants et al., 2009) and identified the full gene sequences and predicted the mRNA and protein sequences of these markers (supplementary material Appendix S1). RT-qPCR showed that PRDM16 was expressed at higher levels in rope tissue than in gill and muscle tissues (ANOVA, P=0.0005; Fisher's PLSD *post hoc* test: rope *versus* gill, P<0.005; rope *versus* muscle, P<0.0005; Fig. 10A), suggesting that it may be driving adipogenesis in sea lamprey rope tissue. PPARγ, PGC-1, C/EBP and UCP were all expressed in gill, muscle and rope tissues (Fig. 10B–E). These transcription factors and UCP-1 homologs are also found in tissues other than BAT in mammals (Borecký et al., 2001; Emre et al., 2007; Jastroch et al., 2005). Interestingly, necdin was expressed in mature but not in immature male sea lamprey (ANOVA, P<0.05; Fisher's *post hoc* test: mature *versus* immature males, P<0.05; Fig. 10F). This result indicates that adipogenesis may be inhibited in animals with fully developed rope tissue (mature males) but not in the immature dorsal ridge with adipogenesis in progress (immature males).

Phylogenetic and genomic analyses of sea lamprey uncoupling protein

Our extensive search in the sea lamprey draft genomes 2.0 (Libants et al., 2009) and 7.0 (Smith et al., 2013) resulted in two homologs of UCP-2. This is consistent with the notion that UCP-2 may be the prototype of UCPs (Borecký et al., 2001; Emre et al., 2007; Jastroch et al., 2005). The sea lamprey UCP protein sequence contains segments similar to UCP energy transfer protein signatures from various species (Fig. 11). Most UCPs contain three 'energy transfer protein signatures' {P-x-[DE]-x-[LIVAT]-[RK]-X-[LRH]-[LIVMFY] (Borecký et al., 2001)}. The first signature of sea lamprey UCP is similar to UCP1-3 (PLDTAKVRL) combined with part of the first signature for brain mitochondrial carrier protein 1 (BMCP1) (QVQ) (Borecký et al., 2001). This signature sequence is usually followed by tripeptide GΦG (Φ=hydrophobic amino acid residue) in all UCPs (Borecký et al., 2001). In the sea lamprey UCP sequence, two GΦG sequences are present: the first Φ is replaced by a hydrophilic and negatively charged E, and the second GΦG is similar to plant UCPs (Borecký et al., 2001). The second signature of sea lamprey UCP (PTDVVKVRFQAQ) is similar to the second signature of UCP2 (Borecký et al., 2001), followed by two GΦG tripeptides. The third signature of sea lamprey UCP (PVDVVKTRYMNS) is similar to the third signature of UCP2/3

(Borecký et al., 2001). The conserved gene synteny for *Ucp* (supplementary material Fig. S3) was partially observed in the sea lamprey draft genome 2.0 (Libants et al., 2009) and confirmed in draft genome 7.0 (Smith et al., 2013). In addition, a steroid 5α-reductase gene is inserted between the *Elmod2* and *Ucp2* genes (supplementary material Fig. S3), which has not been reported in other species (Borecký et al., 2001; Emre et al., 2007; Jastroch et al., 2005). It would be interesting to look into the thermogenic activities of all UCP members because only UCP-1 has been shown to be thermogenic in mammals under physiological conditions (Cannon and Nedergaard, 2004). Further analyses of sea lamprey UCP may also shed light on UCP protein evolution.

Transcriptomic analyses of sea lamprey rope tissue

The presence of the aforementioned biomarkers in the rope tissue prompted us to determine whether the rope tissue transcriptome shows characteristics expected of a thermogenic fat. We sequenced and compared the transcriptomes of rope, gill and muscle tissues of mature male sea lamprey (Fig. 12). From the gill tissue, there were 24,646,140 sequence reads (75 mers), and 58.7% of them passed the quality filter (14,478,560 reads). From the rope tissue, 24,266,464 reads were sequenced and 57.5% of them passed the quality filter (13,958,294 reads). The muscle tissues produced 24,134,527 reads, and 61.4% of them passed the quality filter (14,813,224 reads). These sequences were assembled and aligned to a total of 2766 genes, and these genes were clustered into 1575 GO categories. The transcriptomes of the rope and muscle tissues had 589 genes showing differential expression (1.414× difference) and clustered into 21 GO categories, most of which are related to electron transport chain and energy production (Fig. 7B). The transcriptomes of the rope and gill tissues had 943 genes showing differential expression and clustered into 121 GO categories (Fig. 12A). As expected, the genes involved in fat cell differentiation were upregulated [Fisher's exact test, rope *versus* gill, P=0.01, false discovery rate (FDR)=0.09; Fig. 12) whereas those involved in oxidative phosphorylation (Fisher's exact test, rope *versus* muscle, fisher exact test, $P=9.4\times10^{-7}$, FDR=0), electron transport from NADH to ubiquinone (respiratory complex I; Fisher's exact test, rope *versus* muscle, $P=1.3\times10^{-5}$, FDR=0), and electron-transport-coupled ATP synthesis (Fisher's exact test, rope *versus* muscle, $P=8.3\times10^{-6}$, FDR=0) were downregulated in the rope tissue (Fig. 12).

DISCUSSION

We believe that the rope tissue found in mature male sea lamprey is a unique primordial thermogenic adipose tissue, but not BAT, based on the following reasons. (1) There is no UCP-1, a BAT marker, in the transcriptome of this adipose tissue. Instead, UCP-2, which is universal in various tissues, is present in this adipose tissue. (2) This adipose tissue contains a slightly different set of transcription factors involved in adipogenesis such as CtBP1/2, GRIP1, RBL1, PRDM16, PPARγ and PGC-1α. Specifically, it does not contain Myf5, which dictates the cell lineage of brown adipocytes and muscles. Other factors such as BMP1, BMP3 and UCP-2 are not found in mammalian BAT. (3) The rope tissue appears only in mature male sea lamprey but not in other lamprey species. Therefore, it seems to be an isolated incidence during evolution. (4) The developmental process of the rope tissue is associated with increased NA and the male sex steroid androstenedione. (5) The rope tissue does not contain enriched blood vessels. The minute amount of heat generated is not likely to transmit through the aquatic environment or circulate throughout the body. It more likely acts *via* body contact and serves important functions in sea lamprey reproduction and species identity, but not in cold-induced nonshivering thermogenesis as in mammalian BAT.

One interesting feature of sea lamprey rope tissue is the bias toward downregulated respiratory complex I as shown in the transcriptome. Electrons generated from various metabolic pathways enter the electron transport system or branched electron transport chain at four separate sites that converge in the reduction of coenzyme Q (Efremov et al., 2010). Metabolism of different substrates results in electron donation to specific complexes or sites (Efremov et al., 2010). Oxidation of glutamate, malate and pyruvate provides NADH for electron entry at complex I. β-oxidation of fatty acyl-CoAs generates electrons for entry at complex I or complex II by way of acetyl-CoA metabolism through the tricarboxylic acid cycle (Efremov et al., 2010). This bias in sea lamprey rope tissue may reflect an evolved strategy of energy expenditure at a life stage when the animal has been fasting for quite some time and therefore has a tight budget for carbohydrate metabolism through the

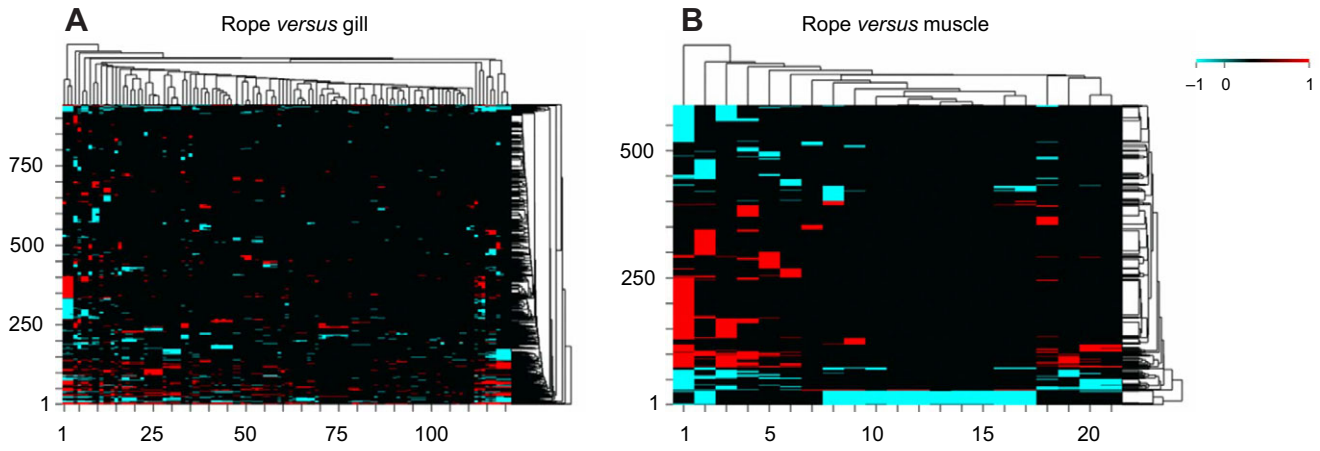

Fig. 12. Heat maps showing different gene expression patterns (color scale represents the fold change) using gene ontology (GO) analyses to compare the transcriptomes of the rope *versus* gill (A; P<0.05, false discovery rate ≤0.1) or muscle tissues (B; P<0.05, false discovery rate ≤0.1) in mature male sea lamprey. Transcriptomes were obtained using Illumina mRNA-Seq sequencing technology. *x*-axis represents the GO categories and *y*-axis represents gene clusters (see supplementary material Appendix S1). Color scale represents the $\log_2$(transcript number in rope/transcript number in gill or muscle). Note that the figure only shows genes with at least 1.414× differential expression level [$\log_2(1.414)=0.5$].

respiratory complex I (the main entrance for carbohydrate). However, fatty acid in the rope tissue can still enter the electron transport chain through respiratory complex II.

It is curious that male sea lamprey, an ectothermic animal, develop a thermogenic secondary sexual character at the final stage of their life span. Many male vertebrates invest a large amount of energy in sexual advertisement, especially in various forms of exaggerated secondary sexual characters (Clutton-Brock, 2007; Ptacek, 2000). As in other male sexual characters, androgen treatment increases the rope size in adult male sea lamprey (Bryan et al., 2007). The rope may simply be an ornamental display, albeit very energy consuming. However, the instant heat produced in the rope by the presence of a sexually mature female and the contact between the rope and female urogenital pore suggest a more active role of the rope tissue. Sea lamprey is the only lamprey species with the rope tissue (Kott et al., 1988), and the only known species outside of the mammalian clade to possess a thermogenic fat. The origin of the rope tissue may have been driven by sexual selection, which would lead to reproductive isolation and speciation (Clutton-Brock, 2007; Ptacek, 2000). This differs from mammalian BAT, which appeared in parallel with homeothermy and nonshivering thermogenesis (Cannon and Nedergaard, 2004). These two thermogenic fats present an extraordinary example of convergent evolution, which resulted in two structures with similar thermogenicity.

ACKNOWLEDGEMENTS

We thank Scot Libants and Drs Peter J. Davidson, Heather L. Eisthen, Richard W. Hill, Brian F. Lantry, Charles P. Madenjian and Shinya Yuge for critical discussions and reading of earlier versions of the manuscript. We thank Ralph Commons and Dr Alicia Pastor for their technical assistance in TEM. We thank Valencia D. Rilington for her help with sample submission to the Research Technology Support Facility at MSU. We also thank Tyler Buchinger and Hanna Kruckman for their technical support. This article is Contribution 1734 of the US Geological Survey Great Lakes Science Center.

AUTHOR CONTRIBUTIONS

Y.-W.C.-D. and W.L. conceived the hypotheses, designed the study and prepared the manuscript. Y.-W.C.-D. performed all the experiments and data analyses. N.S.J. collected rope tissue samples for histology and electron microscopy. K.L. performed the GC-MS. C.-Y.Y. helped with the mitochondrial cytochrome *c* oxidase and ATP assays, temperature measurements and behavioral recordings. C.O.B. helped with the temperature measurements and behavioral recordings. C.P. and J.C. provided assistance and the model for temperature measurements. K.G.N. and C.T.B. provided the computational assistance for GO analyses. M.B.B. performed the AD treatment on immature male sea lamprey. All authors discussed the results and commented on the manuscript.

COMPETING INTERESTS

No competing interests declared.

FUNDING

This study is supported by grants from the Great Lakes Fishery Commission, the US National Institute of General Medical Sciences (grant number 5R24GM83982) and the US National Science Foundation (grant number IOB 0517491) to W.L. Deposited in PMC for release after 12 months.

REFERENCES

Applegate, V. C. (1950). *Natural History of the Sea Lamprey (Petromyzon marinus) in Michigan*. Ann Arbor, MI: University of Michigan.

Block, B. A. (1987). Billfish brain and eye heater: a new look at nonshivering heat production. *News Physiol. Sci.* **2**, 208-213.

Borecký, J., Maia, I. G. and Arruda, P. (2001). Mitochondrial uncoupling proteins in mammals and plants. *Biosci. Rep.* **21**, 201-212.

Bryan, M. B., Scott, A. P. and Li, W. (2007). The sea lamprey (*Petromyzon marinus*) has a receptor for androstenedione. *Biol. Reprod.* **77**, 688-696.

Cannon, B. and Nedergaard, J. (2004). Brown adipose tissue: function and physiological significance. *Physiol. Rev.* **84**, 277-359.

Chung-Davidson, Y.-W., Rees, C. B., Bryan, M. B. and Li, W. (2008). Neurogenic and neuroendocrine effects of goldfish pheromones. *J. Neurosci.* **28**, 14492-14499.

Clutton-Brock, T. (2007). Sexual selection in males and females. *Science* **318**, 1882-1885.

Efremov, R. G., Baradaran, R. and Sazanov, L. A. (2010). The architecture of respiratory complex I. *Nature* **465**, 441-445.

Emre, Y., Hurtaud, C., Ricquier, D., Bouillaud, F., Hughes, J. and Criscuolo, F. (2007). Avian UCP: the killjoy in the evolution of the mitochondrial uncoupling proteins. *J. Mol. Evol.* **65**, 392-402.

Farmer, S. R. (2008). Brown fat and skeletal muscle: unlikely cousins? *Cell* **134**, 726-727.

Gesta, S., Tseng, Y.-H. and Kahn, C. R. (2007). Developmental origin of fat: tracking obesity to its source. *Cell* **131**, 242-256.

Hansen, J. B. and Kristiansen, K. (2006). Regulatory circuits controlling white versus brown adipocyte differentiation. *Biochem. J.* **398**, 153-168.

Hardisty, M. W. (1979). *Biology of the Cyclostomes*, pp. 272-292. London: Chapman and Hall.

Hardisty, M. W. and Potter, I. C. (1971). *The Biology of Lampreys* **1**, 127-206. New York, NY: Academic Press.

Jastroch, M., Wuertz, S., Kloas, W. and Klingenspor, M. (2005). Uncoupling protein 1 in fish uncovers an ancient evolutionary history of mammalian nonshivering thermogenesis. *Physiol. Genomics* **22**, 150-156.

Kott, E., Renaud, C. B. and Vladykov, V. D. (1988). The urogenital papilla in the Holarctic lamprey (Petromyzontidae). *Environ. Biol. Fishes* **23**, 37-44

Kumar, S. and Hedges, S. B. (1998). A molecular timescale for vertebrate evolution. *Nature* **392**, 917-920.

Langmead, B., Trapnell, C., Pop, M. and Salzberg, S. L. (2009). Ultrafast and memory-efficient alignment of short DNA sequences to the human genome. *Genome Biol.* **10**, R25.

Lepri, S., Livib, R. and Politi, A. (2003). Thermal conduction in classical low-dimensional lattices. *Phys. Rep.* **377**, 1-80.

Li, W., Scott, A. P., Siefkes, M. J., Yan, H. G., Liu, Q., Yun, S.-S. and Gage, D. A. (2002). Bile acid secreted by male sea lamprey that acts as a sex pheromone. *Science* **296**, 138-141.

Libants, S. V., Carr, K., Wu, H., Teeter, J. H., Chung-Davidson, Y.-W., Zhang, Z., Wilkerson, C. and Li, W. (2009). The sea lamprey *Petromyzon marinus* genome reveals the early origin of several chemosensory receptor families in the vertebrate lineage. *BMC Evol. Biol.* **9**, 180.

McDaneld, T. G., Nielsen, M. K. and Miner, J. L. (2002). Uncoupling proteins and energy expenditure in mice divergently selected for heat loss. *J. Anim. Sci.* **80**, 602-608.

Mozo, J., Emre, Y., Bouillaud, F., Ricquier, D. and Criscuolo, F. (2005). Thermoregulation: what role for UCPs in mammals and birds? *Biosci. Rep.* **25**, 227-249.

Ohno, T., Furuyama, F. and Kuroshima, A. (2001). Fatty acid composition of brown adipose tissue in genetically heat-tolerant FOK rats. *Int. J. Biometeorol.* **45**, 41-44.

Ptacek, M. B. (2000). The role of mating preferences in shaping interspecific divergence in mating signals in vertebrates. *Behav. Processes* **51**, 111-134.

Seale, P., Kajimura, S., Yang, W., Chin, S., Rohas, L. M., Uldry, M., Tavernier, G., Langin, D. and Spiegelman, B. M. (2007). Transcriptional control of brown fat determination by PRDM16. *Cell Metab.* **6**, 38-54.

Shu, D.-G., Luo, H.-L., Morris, S. C., Zhang, X.-L., Hu, S.-X., Chen, L., Han, J., Zhu, M., Li, Y. and Chen, L.-Z. (1999). Lower Cambrian vertebrates from south China. *Nature* **402**, 42-46.

Smith, J. J., Kuraku, S., Holt, C., Sauka-Spengler, T., Jiang, N., Campbell, M. S., Yandell, M. D., Manousaki, T., Meyer, A., Bloom, O. E. et al. (2013). The lamprey genome: illuminating vertebrate origins. *Nat. Genet.* **45**, 415-421.

Tamura, K., Dudley, J., Nei, M. and Kumar, S. (2007). MEGA4: Molecular Evolutionary Genetics Analysis (MEGA) software version 4.0. *Mol. Biol. Evol.* **24**, 1596-1599.

Weinstein, J. N., Myers, T. G., O'Connor, P. M., Friend, S. H., Fornace, A. J., Jr, Kohn, K. W., Fojo, T., Bates, S. E., Rubinstein, L. V., Anderson, N. L. et al. (1997). An information-intensive approach to the molecular pharmacology of cancer. *Science* **275**, 343-349.

Zeeberg, B. R., Feng, W., Wang, G., Wang, M. D., Fojo, A. T., Sunshine, M., Narasimhan, S., Kane, D. W., Reinhold, W. C., Lababidi, S. et al. (2003). GoMiner: a resource for biological interpretation of genomic and proteomic data. *Genome Biol.* **4**, R28.